Slag Foaming: Fundamentals, Experimental Evaluation and Application in the Steelmaking Industry

A. P. Luz, T. A. Ávila, P. Bonadia, V. C. Pandolfelli

The slag foaming process is currently applied to some equipment for steel production (i.e., electric arc furnace (EAF), basic oxygen furnace (BOF), etc.) aiming to save energy, improve productivity, enhance the refractory service life and inhibit steel re-oxidation. However, the correct control and optimization of the foam generation on the slag surface are still limited and some factors such as basicity, FeO concentration, surface tension, viscosity and how the suspended second phase particles in the liquid act directly in the slag foaming behaviour, need some further understanding. Therefore, this work addresses the main factors that induce foaming, experimental tests used for its evaluation and the use of thermodynamic data in order to control the slag composition while the equipment is being operated. Considering the data presented in the scientific literature, there are various conditions and situations to be explored and thermodynamic calculations seem to be the most suitable tool for these investigations.

1 Introduction

For decades, slag has been considered as a residue of the steelmaking process. However, this material plays an important role due to its capacity to withdraw impurities and inclusions from the steel, reduce energy losses and refractory wearing, and protect steel from re-oxidation [1]. The slag composition (usually in the system of $CaO-MgO-SiO_2-FeO-Al_2O_3$) directly affects its viscosity, thermal conductivity, density and other properties, causing an impact on the ability of the slag to remove impurities from the molten metal and to save energy. Slag foaming has been widely investigated in electric arc furnaces (EAF), basic oxygen furnaces (BOF), etc. [2–7].

This practice protects the refractory materials from the high heat intensity (radiation) generated by the electric arc, improving productivity and energy efficiency of the equipment. It has also been reported [8, 9] that the slag foaming process can save 3–10 % and 25 to 63 % of energy and refractory consumption, respectively.

There are basically two requirements for foaming:

- reactions or processes that generate small gas bubbles and
- suitable slag properties to keep the bubbles as stable foam [10, 11].

Usually, gases resulting from chemical reactions tend to foam the slag with smaller bubbles, whereas the injection of gas phases (oxygen, argon, etc.) results in larger bubbles and less stable foams [12].

The foaming phenomenon can take place by injecting oxygen and carbon into the electric furnace bath (Fig. 1), leading to FeO generation in the liquid (Eq. 1). This phase is one of the major components in the slag, attaining values higher than 20 mass-% [10].

$$Fe_{(l)} + \frac{1}{2} O_{2(g)} \rightarrow FeO_{(l)} \quad (1)$$

After that, carbon reacts with FeO from the liquid, generating $CO_{(g)}$, which is mainly responsible for the foaming effect (Eq. 2) [7].

$$FeO_{(s,l)} + C_{(s,l)} \rightarrow Fe_{(l)} + CO_{(g)} \quad (2)$$

$CO_{(g)}$ formation is also related to the reaction between C (from the metal) and oxygen, as shown by Eq. 3.

$$C_{(l)} + \frac{1}{2} O_{2(g)} \rightarrow CO_{(g)} \quad (3)$$

Reaction 2 prevails at the slag-metal and slag-carbon interfaces, whereas reactions 1 and 3 will take place mainly at the contact area between oxygen and metal. Additionally, the following transformations (Eq. 4 and 5) are expected to occur at the slag-gas and carbon-gas interfaces, respectively [7].

$$FeO_{(l)} + CO_{(g)} \rightarrow Fe_{(l)} + CO_{2(g)} \quad (4)$$

$$CO_{2(g)} + C_{(s)} \rightarrow 2CO_{(g)} \quad (5)$$

All of these reactions (Eq. 2–5) are $CO_{(g)}$ and $CO_{2(g)}$ formers and affect the mass transfer among metal, slag, carbon and gas phases, and are considered as a necessary condition for slag foaming. The generated gas is re-

A. P. Luz, V. C. Pandolfelli
Federal University of São Carlos (UFSCar)
Materials Engineering Department
13565-905 *São* Carlos, SP
Brazil

T. A. Ávila, P. Bonadia
Magnesita Refratários S.A.
Research and Development Center (CPqD)
32210-900 Contagem, MG
Brazil

Corresponding author: *V. C. Pandolfelli*
E-mail: vicpando@power.ufscar.br

Keywords: foaming, slag, electric arc furnace (EAF), thermodynamic simulations

Received: 16.08.2010
Accepted: 02.01.2011

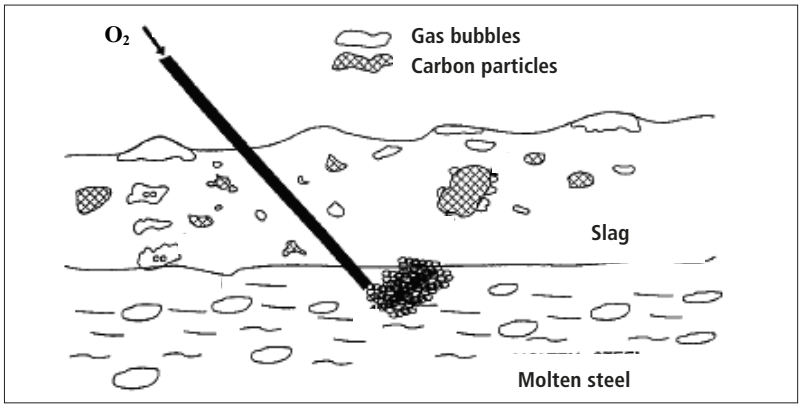

Fig. 1 Sketch of the transformations that take place in EAF equipment during the slag foaming procedure [7]

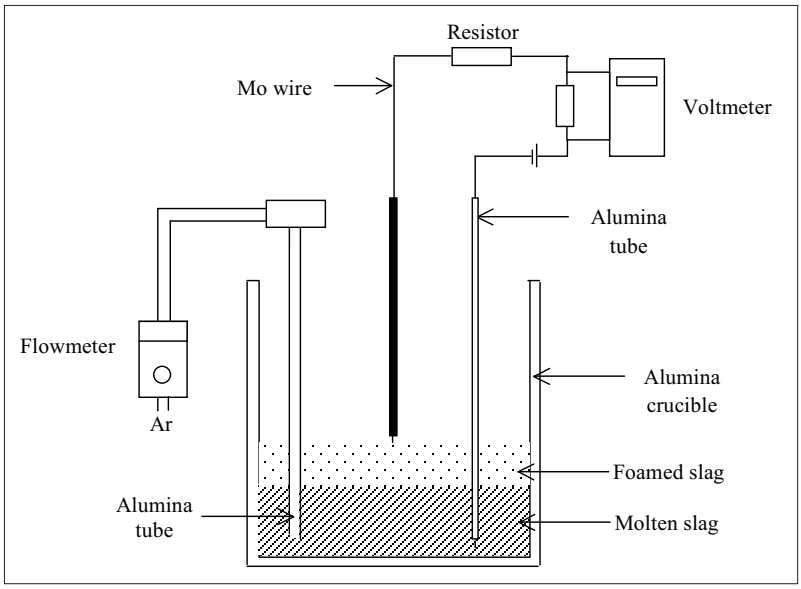

Fig. 2 Experimental apparatus used to measure the slag height when gas is injected into the molten slag [19]

sponsible for the bubbles and foam formation, which should remain at the upper liquid surface, even after the reaction between FeO and C is completed. Thus, the $CO_{(g)}$ formation is related to various process variables, such as size, type and mass flow rate of carbonaceous material, flow rate of oxygen, carbon content in the bath, slag composition, slag-metal interfacial area, etc. [7]. However, despite the well known benefits of slag foaming, few steel producers have managed to generate a consistent foamy practice due to the lack of slag chemistry and viscosity control in the electric arc furnace operation [10].

2 Foaming evaluation

Various authors experimentally evaluated the slag foaming phenomenon, but most of them only focused on the foam height analyses when an inert gas or oxygen was injected into the liquid [3, 12–20]. Fig. 2 shows a schematic drawing of a device (which was adapted in an electric furnace) developed to evaluate the slag foamability at high temperatures. Nevertheless, this procedure only considers the liquid behaviour, not taking into account the interaction between the molten liquid and the refractory, as observed during the EAF operation in the steelmaking process. The foaming index and foam life time are the two parameters that can be attained in this simplified test.

2.1 Foaming index (Σ)

The foaming index or the average travelling time of the gas in the generated foam is attained by the ratio between the change of the slag height – h [cm] and the superficial gas velocity – V_g^s [cm/s]. This parameter is directly related to some of the slag physical properties, such as viscosity, surface tension and density. Fig. 3 and Eq. 6 and 7 are presented to better explain how to evaluate the foaming index [14].

(6)

(7)

where, Q_g [cm³/s] is the gas flow rate, A is the cross-section area of the crucible [cm²], and h [cm] is the change of the slag height. Moreover, the superficial gas velocity and foam height [h] is related to the foam void fraction (α) (Eq. 8 and 9).

(8)

(9)

where, V_g [cm/s] is the actual gas velocity and L [cm] the foam layer thickness. Considering that α value is between 0.7 and 0.9 in any position that the foam has been measured [15], it is possible to assume that the void fraction is constant. Therefore, the foaming index can be expressed in terms of the foam layer thickness and the actual gas velocity (Eq. 10).

(10)

2.2 Foam life time (τ)

The time needed to reduce the foam height from h_0 (initial height) to a specific position h, after halting the gas injection in the studied system, corresponds to the foam life time. Equation 11 describes this parameter and τ is related to the changes between the injected gas and the generation and drainage of the foam [14].

(11)

where, t is the time [s] measured during the foam height reduction. Therefore, for an ideal system (i.e., for which α is constant) the

foaming index will be equal to the average foam life, as follows:

(12)

where, V^{foam} is the foam volume. Simplifying Eq. 12, the τ and Σ correlation can be obtained:

(13)

2.3 Mathematical models

Although various investigations are based on the Σ analyses, the use of this parameter is still controversial as the foaming phenomenon depends on several factors which are not considered in Eq. 10 [16]. Some authors state that this index does not correctly describe foaming (in a quantitative manner) when a chemical interaction between the slag components and the metal takes place at the contact area [13]. Another important aspect is the fact that the linear relationship between L and V_g only exists at high temperatures (> 1500 °C), affecting the evaluation in other experimental conditions.

Thus, having the aim of optimizing and considering the effect of the physical properties of slags on the Σ value, various works focused on the design of mathematical models taking into account some of the main characteristics of the slag (density, viscosity, surface tension or surface tension depression, bubble size of the gas generated in the liquid, etc.).

Ito and *Fruehan* [14, 15] proposed an equation based on dimensional analysis, not considering the presence of solid particles and the bubble size effect in the slag for the $CaO-SiO_2-FeO-Al_2O_3$ system (Eq. 14).

(14)

where, μ = viscosity [Pa·s], γ = surface tension [N·m^{-1}] and ρ = liquid density [kg·m^{-3}]. In this expression, the viscosity is the most important parameter to attain the most suitable Σ value.

Jiang and *Fruehan* [3] adjusted the previous correlation quoted in the former work [14], resulting in more accurate expressions (Eq. 15 and 16). However, this model still presented some limitations and did not make the foaming behaviour for acid slag clear. These observations are associated with the properties of the chosen slag (data collected by experimental tests or inferred from the literature) and also with the use of the surface tension value, instead of the surface tension depression one [16].

(for basic slags) (15)

(for acid slags) (16)

The surface tension depression is the slope of the curve when the surface tension is plotted against the molar concentration of the surface active element, ($\partial\gamma/\partial$ [moles Fe_xO]). *Stadler* et al. [16] stated that the increase of Fe_xO concentration commonly lowers the slag viscosity, leading to a decrease in the foam index. Nevertheless, the surface tension depression (which effect is more significant in the case of acid slag) changes as a function of the Fe_xO concentration and results in the Σ increase, overriding the lowering in the slag viscosity.

Zhang and *Fruehan* [12] suggested expressions similar to the ones obtained by *Jiang* and *Fruehan* also considering the bubble size of the gas formed in the liquid (D_b = average bubble diameter [m]).

(for basic slags) (17)

(for acid slags) (18)

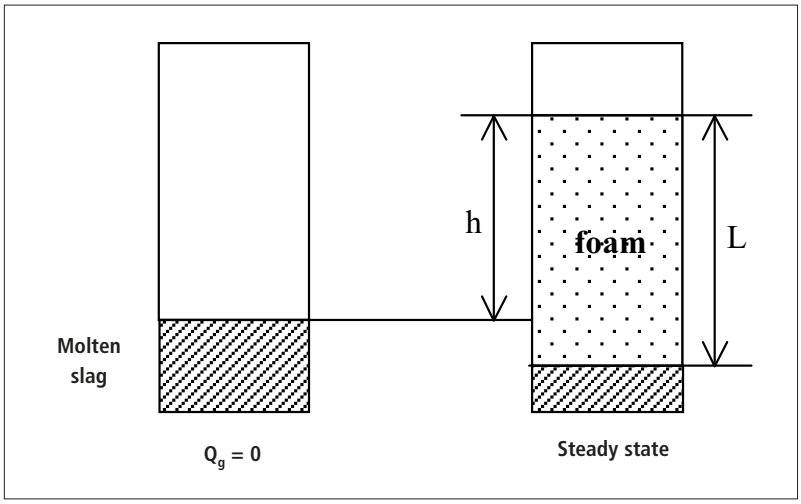

Fig. 3 Sketch of the foaming index measuring procedure [14]

Experimental results obtained after evaluating the slag with $CaO / SiO_2 = 1$ and 5 – 15 mass-% of FeO at 1500 °C, were well correlated and adjusted to this model presented in Eq. 17 and 18. It should be pointed out that the foaming behaviour of basic slag is mainly affected by the viscosity of the liquid, whereas for the acid one it will depend strongly on the average bubble size and surface tension of the liquid [16].

When the bubbles are formed by gas injection, D_b may depend on the liquid viscosity, surface tension, gas flow rate and nozzle geometry [12]. Nevertheless, it is always possible to change the gas bubble size, just by changing the geometry of the blowing nozzle, keeping all the other slag properties constant.

The model proposed by *Zhang* and *Fruehan* [12] is the most accepted and used to describe the slag foamability (based on the measurement of Σ) [3, 11, 13, 14, 16, 18]. However, the correlation presented by *Fruehan* and other authors [12, 14, 15] were developed for a limited range of physicochemical properties and service conditions. Consequently, Eq. 17 and 18 do not predict, in a correct manner, the foam thickness generated in molten slag presenting different properties from those specified in these works.

Ghag et al. [21, 22] showed that the values derived from Eq. 17 have some discrepancies when compared with the results attained in practical tests. Based on their studies, the authors concluded that the liquid viscosity has a significant effect on the gener-

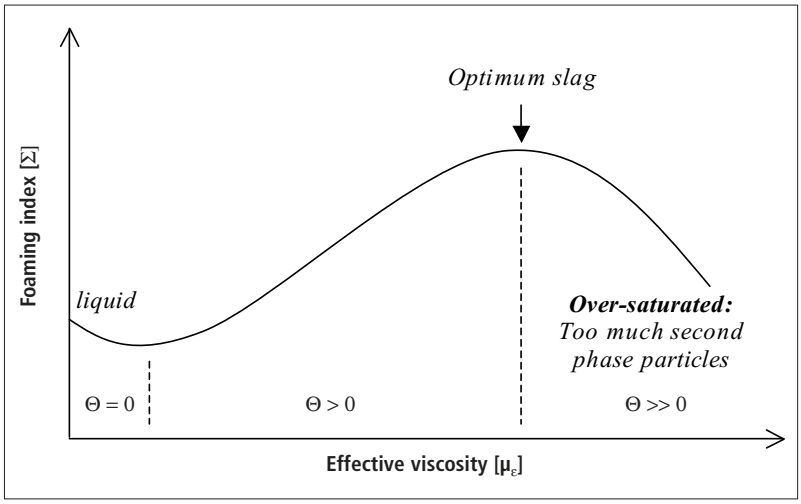

Fig. 4 The relationship between foaming index and effective viscosity [28]

ated foam height and the following correlation was suggested:

(19)

where, E_{ff} is the effective elasticity of the liquid film which forms the bubble and g is the gravitational constant. Despite the advances in the mathematical models, determining the effective elasticity value is difficult and additional parameters are still required. Furthermore, the comparison between the quoted model (Eq. 19) and the slag foaming data presented in the literature has not yet been carried out.

Scientific works commonly consider the injection of a gas phase in the liquid in order to promote slag foaming. However, reactions involving oxygen and carbon (added to the liquid bath) in the electric arc furnace operation lead to the CO bubbles generation, which will be responsible for the foam formed at the top of the molten slag.

Aiming to understand the system changes in order to attain a condition similar to the practical tests, some authors [23] evaluated and suggested a physical model considering a system containing a liquid material comprised by slag and metal. This work attested that the main factors that affect the liquid foamability are the surface tension and viscosity of the slag, interfacial tension between slag-metal and surface tension of the metal phase. Other publications [24–27] also discuss the effectiveness of the existing models presented in the scientific literature, but up to now there is no agreement among them and the slag foaming phenomenon is far from being completely understood.

3 Parameters that affect the slag foaming practice

Slag properties may inhibit or promote the generation of the foam, therefore some of these characteristics are presented and discussed as follows:

3.1 Basicity

The key issue for EAF slag engineering is to attain a balance between the refractory and fluxing oxides in its composition [28]. The refractory oxides such as MgO and CaO can increase the effective viscosity of the slag. On the other hand, SiO_2, Al_2O_3, FeO, MnO and CaF_2 will increase its fluidity and negatively affect the foam generation at the upper surface of the liquid. The slag basicity concept is an attempt to define a balance between the components of the liquid. Some expressions used to described this parameter are [28]:

(20)

3.2 FeO concentration

The iron oxide contained in the slag during the EAF operation is usually formed by the iron oxidation when oxygen is injected into the molten metal. FeO is a major oxide component in slag and has a significant effect on viscosity, foamability, slag volume, productivity and power consumption. Low FeO content (< 10 mass-%) results in a viscous slag which is hard to foam. Conversely, a FeO content > 40 mass-% increases the fluidity and the gas bubbles cannot remain in the liquid. The excessive amount of this oxide can also result in an acid slag, shortening the refractory service life and wasting expensive chemical energy during the steel refining process [8].

3.3 Surface tension

The bubble size increases by increasing the surface tension of slag. Therefore, the film between the bubbles becomes thin, because the void fraction in the foam scales with the bubble size. The drop of the foam height will be induced by the pressure difference as a result of the film surface curvature around the bubble. Thus, the rate of rupture of the bubbles at the upper surface of the foam increases with the surface tension of the slag [18, 23].

3.4 Viscosity

An optimized slag chemical composition (for a chosen temperature) should be attained to assure the formation and stability of the gas bubbles. For a liquid with low viscosity, the bubbles will be easily eliminated and the foam may be suppressed. Conversely, the bubbles will not be generated in a high viscous liquid [9, 23].

3.5 Suspended second phase particles

Their presence in a slag has a much greater impact on foaming than the surface tension and slag viscosity [28]. The solid particles (commonly Ca_2SiO_4 or MgO · FeO) act as gas nucleation sites, leading to a high amount of small gas bubbles in the slag. Additionally, the suspended particles can change the effective slag viscosity, as presented in Eq. 21.

(21)

where, μ_e is the effective viscosity of the slag [Pa·s] and Θ is the fraction of precipitated solid phases ($0 < \Theta < 0.74$). There is a close relationship between the foaming index and the effective viscosity (Fig. 4) and, the higher μ_e, the longer the residence time of the gas bubbles in the slag will be, extending the stability of the foam. However, there is a maximum amount of second phase particles that is beneficial for the foam stability.

Furthermore, other factors such as adding carbon or MgO particles, the temperature of the process, etc., directly affect the foam for-

mation. When a high amount of carbon particles is added to the liquid, slag foaming may be inhibited. It was postulated that when a hydrophobic particle (or material that presents limited wettability, such as carbon) comes into contact with the liquid film, the instantaneous contact angle at the formed three-phase boundary (solid, liquid, gas) is smaller than the equilibrium contact one [29]. This difference results in a driving force that makes the bubble move around the particle, stretches the liquid film and decreases foaming. Thus, a control of the FeO and C contents in the system is required, because the excess of carbon can inhibit foaming instead of inducing the chemical reactions responsible for keeping this process.

The temperature effect in the foaming practice has also been investigated in some studies [19, 30] and the increase of this parameter leads to the decrease in the foaming index. The temperature also acts on the viscosity and chemical saturation of the liquid, affecting the precipitation of second phases. It must be pointed out that the saturated MgO or CaO slag will not only foam better, but will also decrease the refractory wearing of the electric arc furnaces [8].

4 Use of phase diagrams and thermodynamic simulations to predict slag foaming behaviour in EAF

Optimization and control of the slag during the EAF operation is very difficult, because not only molten metal but also scrap is added to the furnace, affecting the liquid composition. Information about the scrap particles size distribution, oxidation level, Si and Al content, etc., is very important to assure the efficiency of the equipment and foaming practice at high temperatures.

Pretorius et al. [28] stated that the control of the slag in conventional EAF operations can be compared to hitting a moving target, because this is a dynamic system which constantly needs to be adjusted to keep a continue and stable foam generation, due to the changes in the slag throughout the steelmaking process.

The easiest way to adjust the slag chemistry in this type of operation consists of injecting carbon or adding limited amounts of MgO or dolomite ($CaMg(CO_3)_2$), allowing the foam to form in the furnace. EAF slag typically contains five major oxides: CaO, MgO, SiO_2, FeO and Al_2O_3. According to practical tests, it is known that the suitable compositions are the MgO saturated ones, containing suspended second-phase particles (i.e., MgO · FeO (magnesio-wustite, MW)) [7]. The MgO saturated liquids not will only positively affect the foaming, but also result in a decrease of the refractory wearing.

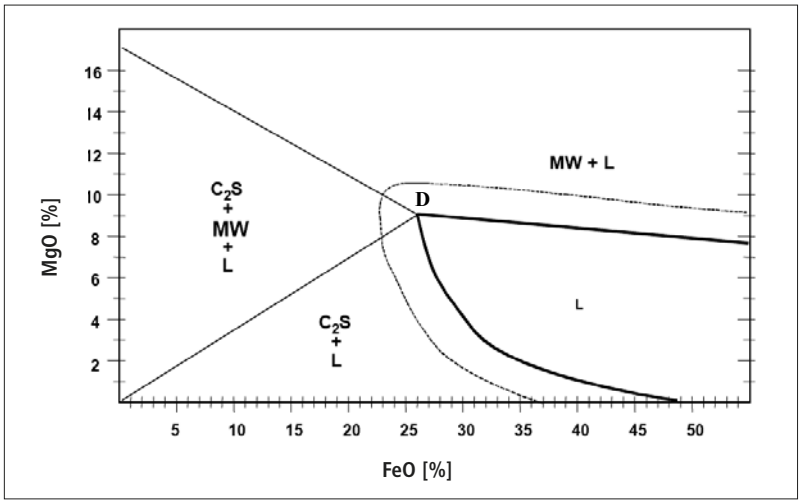

Fig. 5 Isothermal solubility diagram (ISD) of the $FeO-MgO-SiO_2-CaO-Al_2O_3$ system for a basicity B_3 of 2.0 and temperature = 1600 °C [28]; MW = MgO·FeO, C_2S = 2 CaO·SiO_2, L = liquid

Therefore, based on the phase diagrams of the studied system, it is possible to define the influence of each slag component and which combination among them can result in liquid saturation and precipitation of the MgO · FeO phase. Some works suggest the use of the isothermal solubility diagrams (ISD) [1, 5, 7, 28], which are valid for a specific basicity value and express the relationship between the MgO and FeO in mass-%. Fig. 5 shows an example of an ISD diagram for the system $FeO-MgO-SiO_2-CaO-Al_2O_3$ at 1600 °C. Considering the B_3 basicity ratio, these graphs are prepared by analyzing the isothermal sections of the ternary diagrams $MgO-SiO_2-CaO$, $MgO-SiO_2-FeO$, $MgO-CaO-FeO$ and $CaO-SiO_2-FeO$. In addition, the effect of the Al_2O_3 on the MgO solubility can be calculated by the correction factors:

(22)

where, MgO_{ref} [%] corresponds to the MgO content in the CaO-MgO saturated slag (double saturation) at a selected temperature. Conversely, the Al_2O_3 effect is described by the equation:

(23)

Usually, the ISD diagrams (i.e., Fig. 5) are split into 4 regions: liquid slag (L), MgO · FeO (MW) saturated liquid, 2 CaO · SiO_2 (C_2S) saturated liquid and the dual saturated ($L + C_2S + MW$) liquid. Point D is named dual saturated point and the lines delimitating the $L + (MW + L)$ and $L + (L + C_2S)$ regions (highlighted with bold lines in the graph) are known as the MgO and CaO saturated ones, respectively. Moreover, the dashed line surrounding the liquidus region indicates the slag composition with peak foaming performance, where the maximum slag foaming takes place (about 6 mass-% out of L region [5]).

Changing some parameters such as temperature, oxygen partial pressure and slag basicity, will move the saturation lines and the point of dual saturation (D) to a different location in the diagram and the MgO and FeO content of the slag should be re-adjusted to ensure the foaming effect.

One of the most used procedures in an EAF to extend the foamy conditions consists of injecting MgO fines into the slag towards the end of the heating period. Fig. 6 shows two examples – where K and T are the original slag compositions.

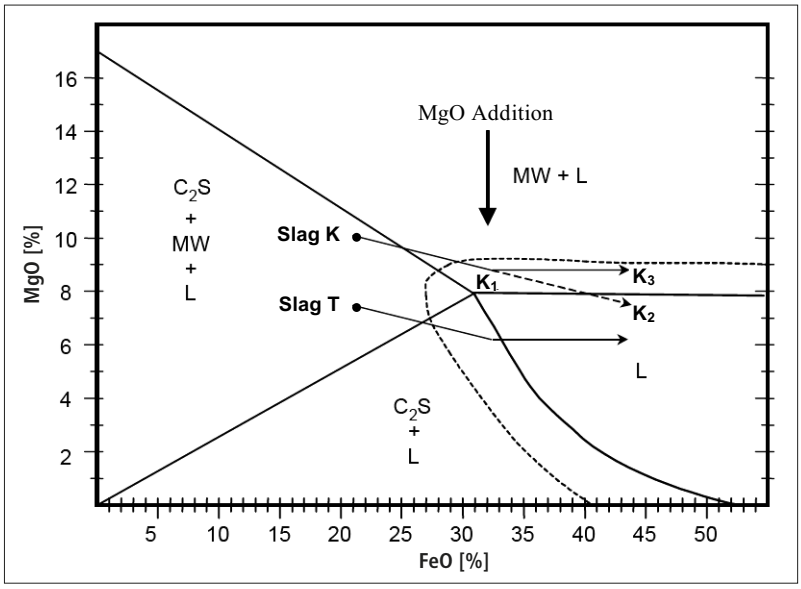

Fig. 6 ISD diagram showing the effect of adding MgO to the path of the liquid composition [28]

As the FeO is generated and composition K moves towards K_2, the fluidity of the slag increases (Fig. 6). Initially the foaming properties of the liquid increases moving from point K to K_1, because the latter is located in the region where the foam generation is favored. Nevertheless, from K_1 to K_2, the slag becomes too liquid (low viscosity) to foam in a suitable way. The MgO fines injection into the slag (addition at point K_1) will change the liquid composition and ensure the presence of second-phase particles, keeping the foamy conditions [28]. In this case, adding MgO aims to attain two main purposes: 1) to reduce the slag temperature by incorporating a material which was previously at room temperature, and 2) to maintain the MgO level due to the FeO increase during the furnace operation.

However, the effectiveness of the MgO or doloma (CaO·MgO) injection into the EAF depends on the initial MgO content in the slag. Considering composition T (Fig. 6), the magnesia level is too low and a further injection of this phase will not result in significant changes.

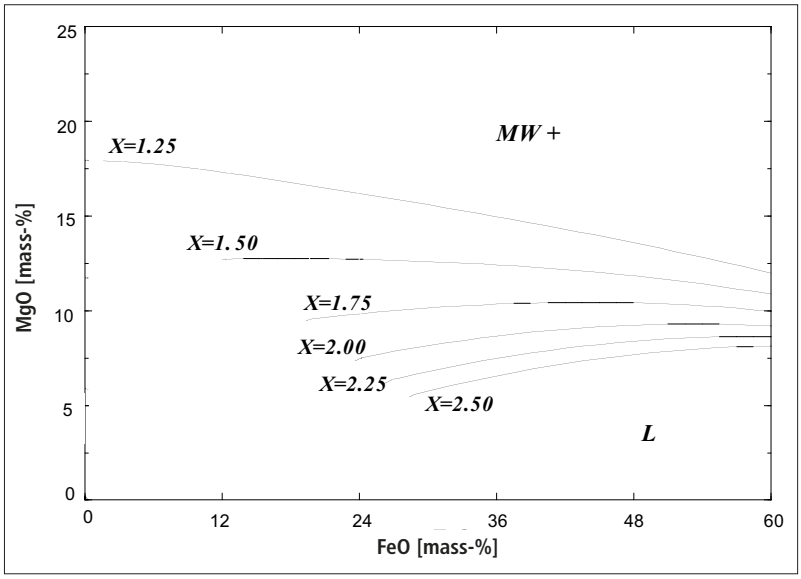

Fig. 7 MgO saturated lines in the FeO–MgO–CaO–SiO_2 system as a function of the slag basicity (CaO/SiO_2 = X), at 1600 °C and high oxygen partial pressure ($pO_2 = 10^{-4,72}$ atm) [7]

The ISD diagram analyzed by *Pretorius* et al. [28] provides important information which helps and indicates which adjustments can be made to extend foaming in the furnace. Nevertheless, some limitations can be detected: 1) only applicable for the analysis of slag basicity (B_3) between 1.2 – 3.5; 2) suitable for FeO values < 55 mass-% and 3) for temperatures between 1500 °C and 1750 °C. Due to these adjustments and correction factors used in the diagrams, some imprecision can still be found when using these graphs.

A better way to obtain such diagrams and also to define the effect of various parameters on the slag characteristics is via thermodynamic software such as FactSage, Thermo-Calc, etc. [7, 8]. Thermodynamic calculations can predict the position of the dual saturation point and the MgO saturated lines as a function of the slag basicity (Fig. 7), temperature, oxygen partial pressure and other parameters. Compared to some mathematical models [7] and phase diagrams, these analyses are very accurate and present an error < 1 % when FeO content in the slag is less than 60 mass-%.

In addition, simulations can be carried out for any chemical compositions and slag basicity values. Considering a practical condition, the liquid basicity is related to the EAF charging materials and directly depends on the cold charge content (scrap and/or solid pig iron) added during the operation. The amount of cold charge is strategic and based on the current price of these materials. Consequently, the scrap and/or solid pig iron additions reduce the slag basicity due to the increase in SiO_2 content in the system and, therefore, the steel plant may operate with B_3 values lower than 1.2 in the slag.

Thus, the use of thermodynamic simulations and the control of the slag compositions during the EAF operation can evaluate some conditions not explored by the scientific literature until today (B_3 < 1).

For example, the ISD diagram for a slag basicity B_3 = 0.9 (25.7 mass-% of CaO, 16.2 mass-% of SiO_2 and 11.6 mass-% of Al_2O_3) can be designed by the FactSage software, using the Phase Diagram module. In this case, MgO, FeO, O_2 and $(CaO)x(SiO_2)y(Al_2O_3)z$ are considered, where x, y and z correspond to the molar stoichiometries of the oxides of the slag. Temperature and oxy-

gen partial pressure of the furnace environment can be easily defined at this calculation step. Fig. 8 shows a diagram prepared using the FactSage software by the authors of this work, for the slag described above ($B_3 = 0.9$), temperature of 1600 °C and $pO_2 = 0.21$.

Significant changes in the diagram were observed when compared with those shown in Fig. 5. For $B_3 < 1$, the precipitation of C_2S and liquid saturation in this phase is not possible, considering the chosen interval (the FeO and MgO content equal to 0 – 60 mass-% and 0 – 25 mass-%, respectively) at 1600 °C. Conversely, slag containing high amounts of FeO can still be saturated by the spinel phase (mainly $FeMg_2O_4$, but it can also contain $MgAl_2O_4$ in its composition – Fig. 8). Therefore, slag with a basicity lower than 1 will show a distinct behaviour at the thermodynamic equilibrium when compared with the one with high basicity values (B_3).

It can be concluded that the data provided by the simulations will help and indicate which adjustments may be carried out during the EAF operation in order to improve and optimize suitable conditions for foaming. There are various conditions and situations to be explored and the thermodynamic calculations seem to be the most suitable tool for these investigations.

5 Final remarks

Based on the various works in the literature and due to the complexity of slag foaming phenomenon, it can be concluded that some difficulties remain to define the best conditions to attain the foam generation and its stability at the upper surface of the molten slag.

Developed mathematical models are usually adjusted to a simple situation where a constant gas flow (inert gas or oxygen) is injected into the liquid. However, the reactions between oxygen and carbon with the molten liquid components and the metal-slag interactions result in changes of the slag properties.

Therefore, some adjustments in the liquid composition are frequently needed. Considering these aspects, the development of isothermal solubility diagrams and the use of thermodynamic simulations seem to be a good option to evaluate the best conditions to generate and maintain the stability of the foam during the EAF operation.

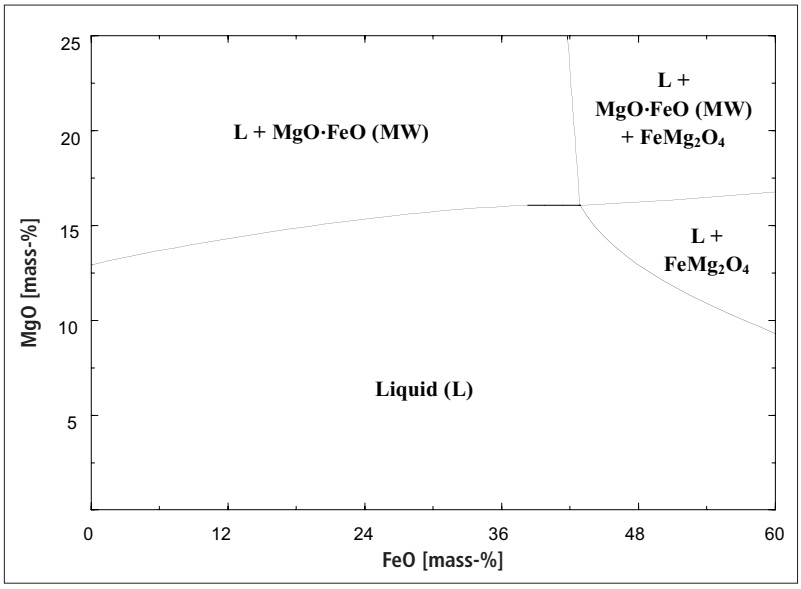

Fig. 8 Phase diagram in the $FeO-MgO-SiO_2-CaO-Al_2O_3$ system for a basicity $B_3 = 0.9$, temperature = 1600 °C and $pO_2 = 0,21$ atm

Acknowledgments

The authors are grateful to the *Conselho Nacional de Desenvolvimento Científico e Tecnológico* (CNPq) and *Magnesita Refratários S.A.* (Brazil) for supporting this research.

References

[1] Ávila, T.A.; Freire, R.S.; Silva, G.F.B.L.; Borges, R.N.: Design of slags compatible with refractory systems. In: Proc. UNITECR 2009, Salvador. Brazil, pp.1–4

[2] Guzzon, M.; Sahajwalla, V.; Memoli, F.; Pustorino, M.: The behaviour of the secondary metallurgy slag into the EAF. How to create a good foamy slag with the appropriate basicity using a mix of lime and recycled ladle slag as EAF slag former. In: Proc. 38th Seminário de Aciaria, Belo Horizonte, Brazil, 2007, pp. 1–12

[3] Jiang, R.; Fruehan, R.J.: Slag foaming in bath smelting. Metallurg. & Mat. Trans. B. 22 (1991) 481–489

[4] Kitamura, S.; Okohira, K.: Influence of slag composition and temperature on slag foaming. ISIJ Inter. 32 (1992) [6] 741–746

[5] Novák, M.; Straka, J.; Pribyl, M.: Influence of the slag foaming process applied in high alloyed steel production on refractory wear of EAF at Pilsen Steel melt shop. In: Proc. UNITECR 2009, Salvador, Brazil, pp. 1–4

[6] Jung, S.M.; Fruehan, R.J.: Foaming characteristics of BOF slags. ISIJ Inter. 40 (2000) [4] 348–355

[7] Morales, R.D.; Rubén Lule, G.; Lopez, F.; Camacho, J.; Romero, J.A.: The slag foaming practice in EAF and its influence on the steelmaking shop productivity. ISIJ Inter. 35 (1995) [9] 1054–1062

[8] Kwong, K.S.; Bennet, J.P.; Krabbe, R.; Petty, A.; Thomas, H.: Thermodynamic calculations predicting MgO saturated EAF for use in EAF steel production. In: Proc. TMS 2009 – 138th Annual Meeting and Exibition, San Francisco. EUA (2009) 63–70

[9] Kwong, K.S.; Bennet, J.P.: Recycling practices of spent MgO-C refractories. J. Min. & Mat. Characterization & Engineering 1 (2002) [2] 69–78

[10] Pretorius, E.B.; Nunnington, R.C.: Stainless steel slag fundaments: from furnace to tundish. Ironmaking and Steelmaking 29 (2002) [2] 133–139

[11] Matsuura, H.; Fruehan, R.J.: Slag foaming in an electric arc furnace. ISIJ Inter. 49 (2009) [10] 1530–1535

[12] Zhang, Y.; Fruehan, R.J.: Effect of the bubble size and chemical reactions on slag foaming. Metallurg. & Mat. Trans. B. 26 (1995) 803-812

[13] Wu, K.; Qian, W.; Chu, S.; Niu, Q.; Luo, H: Behaviour of slag foaming caused by blowing gas in molten slags. ISIJ Inter. 40 (2000) [10] 954–957

[14] Ito, K.; Fruehan, R.J.: Study on the foaming of $CaO-SiO_2-FeO$ slags, Part I: Foaming parameters and experimental results. Metallurg. & Mat. Trans. B. 20 (1989) 509–514

[15] Ito, K.; Fruehan, R.J.: Study on the foaming of $CaO-SiO_2-FeO$ slags, Part II: Dimensional analysis and foaming in iron and steelmaking processes. Metallurg. & Mat. Trans. B. 20 (1989) 515–521

[16] Stadler, S.A.C.; Eksteen, J.J.; Aldrich, C.: An experimental investigation of foaming in acidic, high Fe_xO slags. Min. Engng. 20 (2007) 1121–1138

[17] Ghag, S.S.; Hayes, P.C.; Lee, H.G.: Physical model studies on slag foaming. ISIJ Inter. 38 (1998) [11] 1201–1207

[18] Hara, S.; Kitamura, M.; Ogino, K.: The surface viscosities and the foamines of molten oxides. ISIJ Inter. 30 (1990) [9] 714–721

[19] Ozturk, B.; Fruehan, R.J.; Effect of temperature on slag foaming, Metallurg. & Mat. Trans. B. 26 (1995) 1086–1091

[20] Zhang, Y.; Fruehan, R.J.: Effect of gas type and pressure on slag foaming. Metallurg. & Mat. Trans. B. 26 (1995) 1088–1091

[21] Ghag, S.S.; Hayes, P.C.; Lee, H.G.; Model development of slag foaming. ISIJ Inter. 38 (1998) [11] 1208–1215

[22] Ghag, S.S.; Hayes, P.C.; Lee, H.G.: The prediction of gas residence times in foaming $CaO\text{-}SiO_2\text{-}FeO$ slags. ISIJ Inter. 38 (1998) [11] 1216–1224

[23] Ogawa, Y.; Huin, D.; Gaye, H.; Tokumitsu, N.: Physical model of slag foaming. ISIJ Inter. 33 (1993) [1] 224–232

[24] Hong, L.; Hirasawa, M.; Sano, M.: Behaviour of slag foaming with reduction of iron oxide in molten slags by graphite. ISIJ Inter. 38 (1998) [2] 1339–1345

[25] Lotun, D.; Pilon, L.: Physical modeling of slag foaming for various operating conditions and slag compositions. ISIJ Inter. 45 (2005) [6] 835–840

[26] Misra, P.; DeO, B.; Chhabra, R.P.: Dynamic model of slag foaming in oxygen steelmaking converters. ISIJ Inter. 38 (1998) [11] 1225–1232

[27] Kim, H.S.; Min, D.J.; Park, J.H.: Foaming behaviour of $CaO\text{-}SiO_2\text{-}FeO\text{-}MgO_{sat}\text{-}C$ (X = Al_2O_3, MnO, P_2O_5 and CaF_2) slags at high temperatures. ISIJ Inter. 41 (2001) [4] 317–324

[28] Pretorius, E.B.; Carlisle, R.C.: Foamy slag fundamentals and their practical application to electric furnace steelmaking. 56th Electric Furnace Conf. ISS-15-18, New Orleans/USA, 1998, pp. 275–291

[29] Zhang, Y.; Fruehan, R.J.: Effect of carbonaceous particles on slag foaming. Metallurg. & Mat. Trans. B. 26 (1995) 813–819

[30] Sedivy, C.H.; Krump, R.: Tools for foaming slag operation at EAF steelmaking. Arch. Metallurgy & Mat. 53 (2008) [2] 409–413